The American Journal of Human Genetics, Volume *108*

Supplemental information

Association of structural variation

with cardiometabolic traits in Finns

Lei Chen, Haley J. Abel, Indraniel Das, David E. Larson, Liron Ganel, Krishna L. Kanchi, Allison A. Regier, Erica P. Young, Chul Joo Kang, Alexandra J. Scott, Colby Chiang, Xinxin Wang, Shuangjia Lu, Ryan Christ, Susan K. Service, Charleston W.K. Chiang, Aki S. Havulinna, Johanna Kuusisto, Michael Boehnke, Markku Laakso, Aarno Palotie, Samuli Ripatti, Nelson B. Freimer, Adam E. Locke, Nathan O. Stitziel, and Ira M. Hall

Supplemental Figures

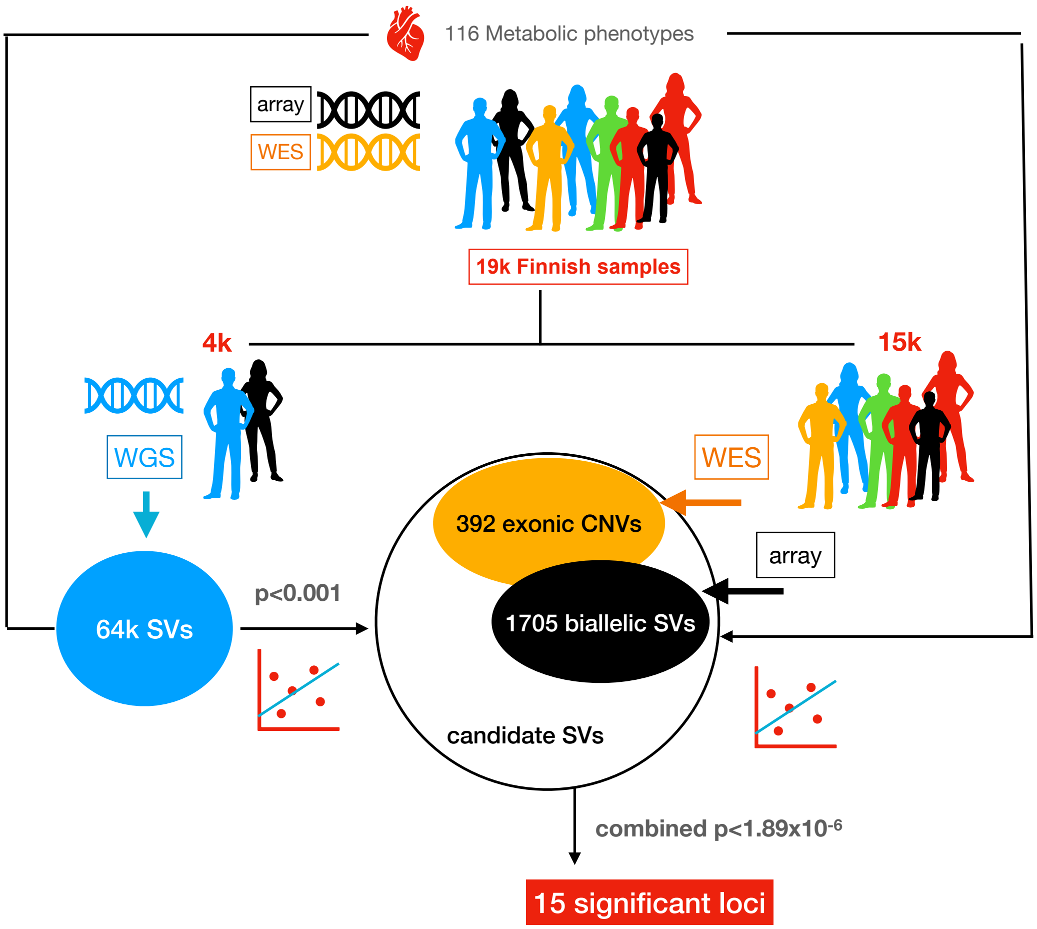

Figure S1. Flowchart of the overall experimental design.

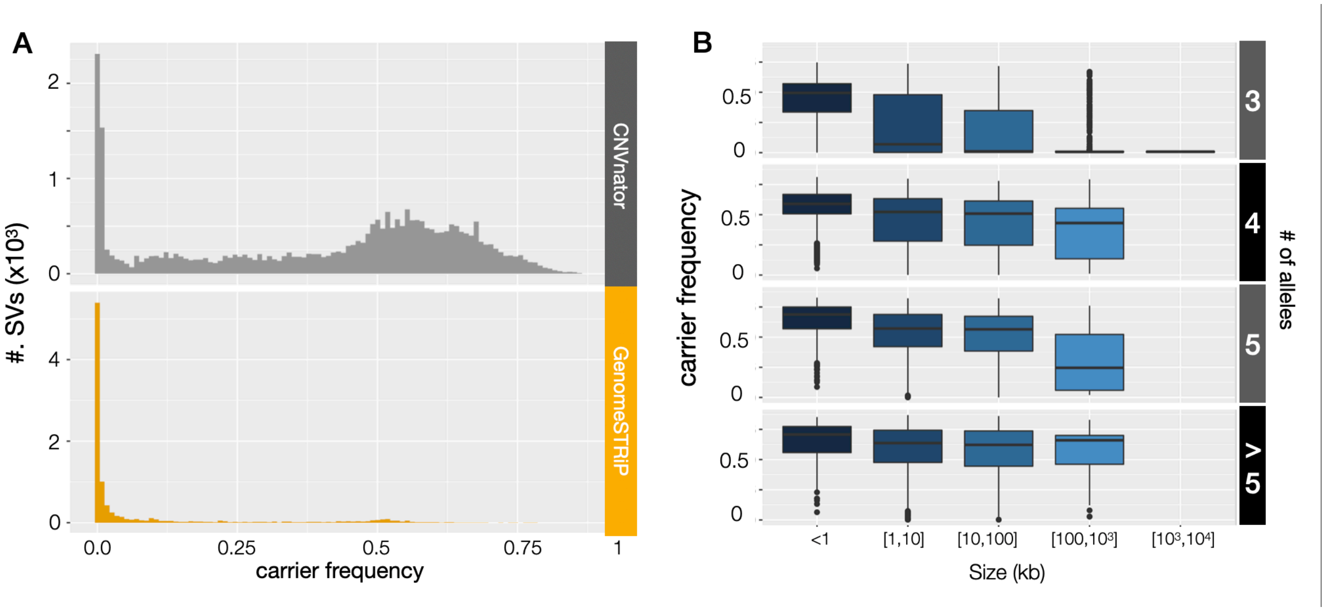

Figure S2. **(A)** The carrier frequency spectrum of multi-allelic CNVs, stratified by detection methods. Note that the concentration of CNVnator variants between 0.5-0.75 were primarily caused by large segmental duplication regions near centromeres and telomeres, where the variant boundaries were challenging to define and the CNVs were detected in highly fragmented form. Such regions are often excluded from genetic analysis but were included here to maximize sensitivity. **(B)** Similar frequency distribution to (A), stratified by mCNV size groups. The central line and box borders represent median, 1st and 3rd quartiles. The upper whiskers extend to the lesser extreme of the maximum and the 3rd quartile plus 1.5 times the interquartile range (IQR); the lower whiskers extend to the lesser extreme of the minimum and the 1st quartile minus 1.5 times the IQR.

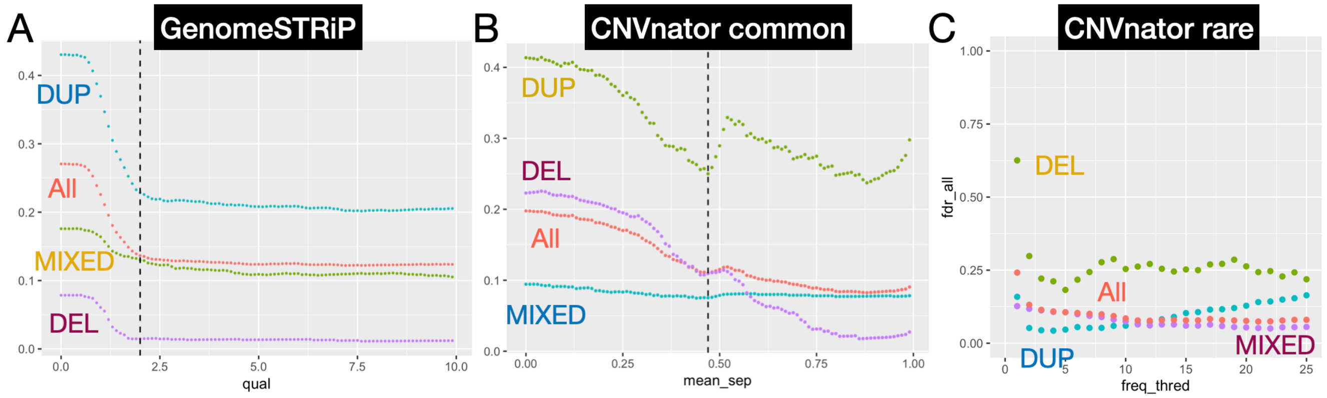

Figure S3. FDR curves under different quality thresholds for **(A)** GenomeSTRiP CNVs, **(B)** Common variants of CNVnator CNVs, and **(C)** Rare variants of CNVnator CNVs. The FDR was estimated from the array intensity data of METSIM samples using IntensityRankSumAnnotator from the GenomeSTRiP pipeline, among CNVs covered by at least two probes. GenomeSTRiP CNVs were filtered based on the "GSCNQUAL" score output by the software, common CNVnator CNVs were filtered by the "mean_sep" metrics from the constrained GMM model, and the rare CNVnator CNVs were filtered by carrier frequency. The results are presented for all variants as well as by different variant types, indicated by the colors shown.

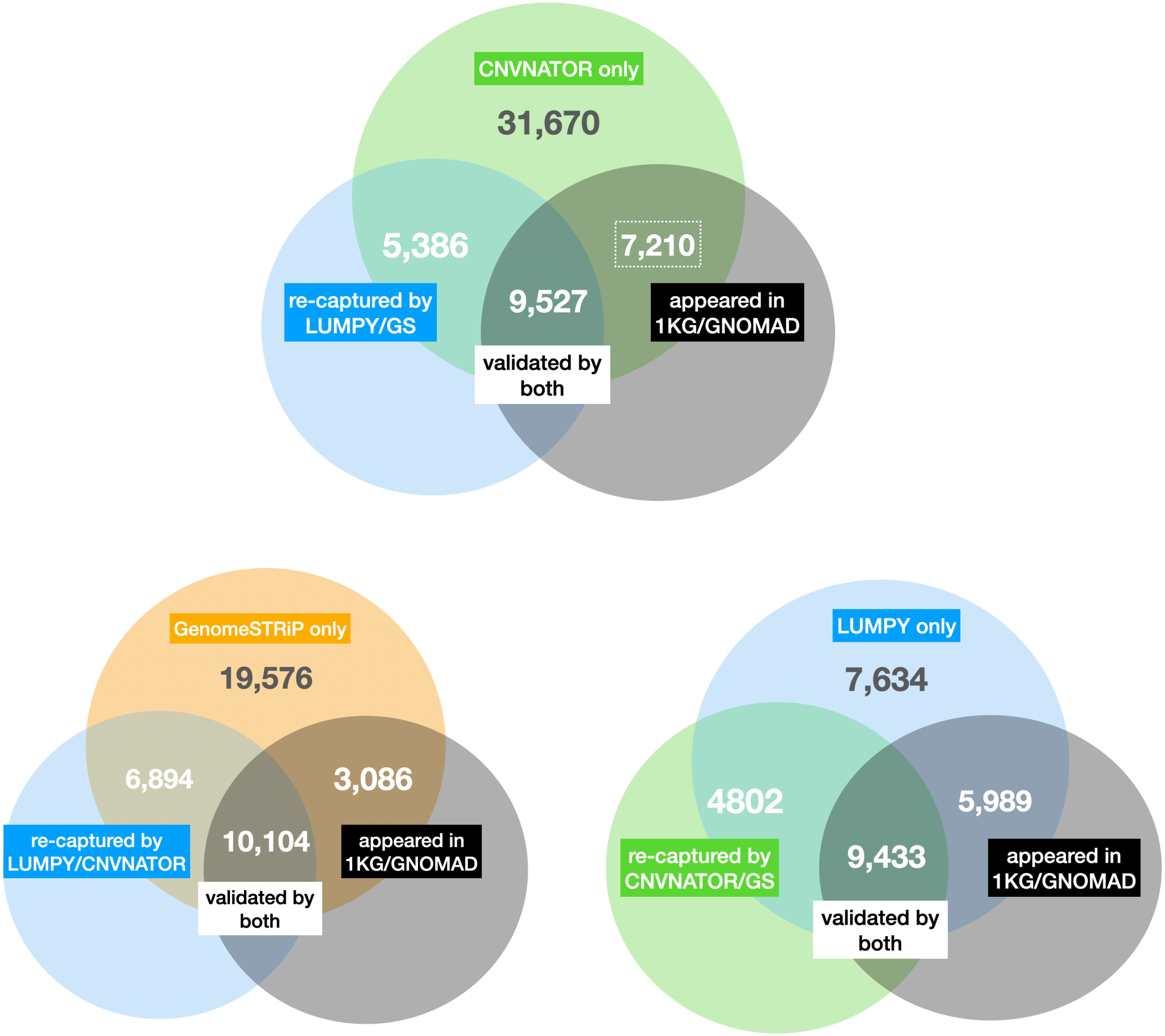

Figure S4. For each of the three SV detection methods used in this study, these venn diagrams show the number of CNVs that were also identified by the other two "internal" pipelines used in this study (left), and the "external" reference SV callsets from 1KG and gnomAD (right). The upper part of each diagram also shows the number of CNVs only identified by a given pipeline. Dashed rectangles were used to emphasize the number of CNVnator CNVs that were validated by external callsets but missed by the other two pipelines, showing the complementary nature of the methods used for this study. 50% reciprocal overlap was used to compare CNV calls from different callsets.

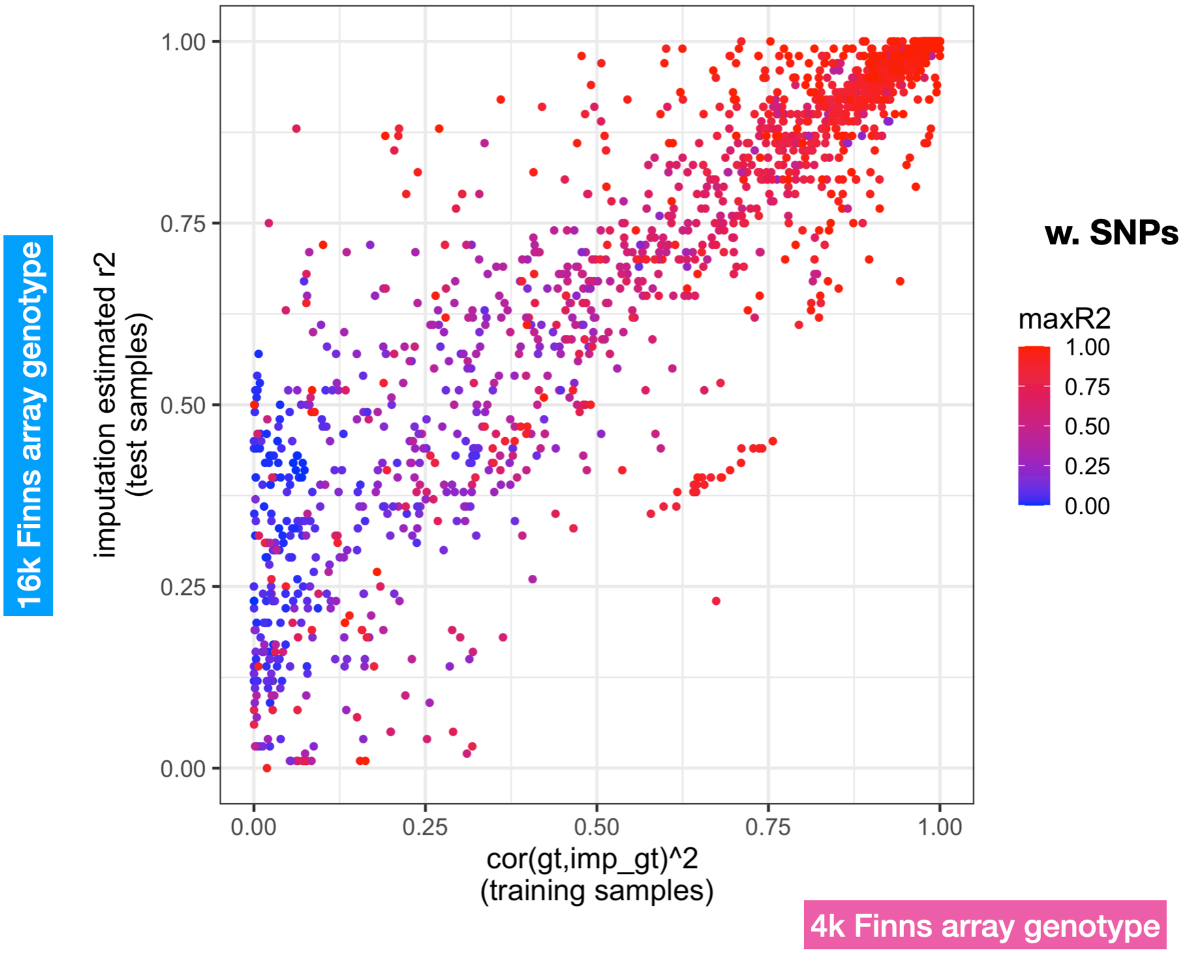

Figure S5. The overall evaluation of imputation quality with two metrics. The Y-axis shows the Beagle output quality score (DR2) for the ~15k tested samples, which is the estimated correlation between the imputed genotype and real genotype for each variant, and the X-axis shows the “training error” for the ~4k samples with WGS data. Training error was calculated using the WGS data as reference and array data as test input, after which the correlation of real genotype (based on WGS) and predicted genotype was calculated. The color shows how well each SV was tagged by nearby SNPs located within 1 Mb.

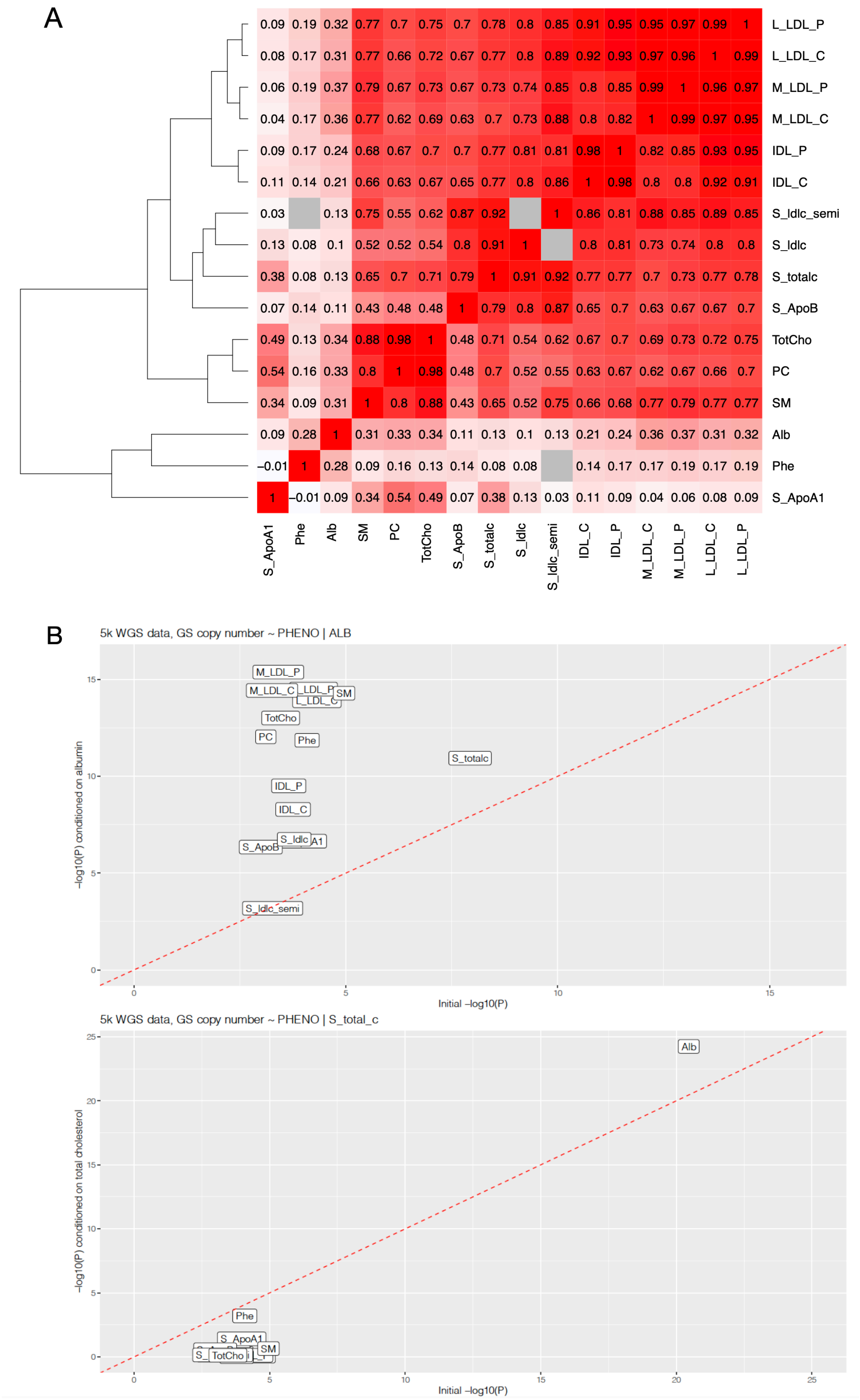

	S_ApoA1	Phe	Alb	SM	PC	TotCho	S_ApoB	S_totalc	S_ldlc	S_ldlc_semi	IDL_C	IDL_P	M_LDL_C	M_LDL_P	L_LDL_C	L_LDL_P
L_LDL_P	0.09	0.19	0.32	0.77	0.7	0.75	0.7	0.78	0.8	0.85	0.91	0.95	0.95	0.97	0.99	1
L_LDL_C	0.08	0.17	0.31	0.77	0.66	0.72	0.67	0.77	0.8	0.89	0.92	0.93	0.97	0.96	1	0.99
M_LDL_P	0.06	0.19	0.37	0.79	0.67	0.73	0.67	0.73	0.74	0.85	0.8	0.85	0.99	1	0.96	0.97
M_LDL_C	0.04	0.17	0.36	0.77	0.62	0.69	0.63	0.7	0.73	0.88	0.8	0.82	1	0.99	0.97	0.95
IDL_P	0.09	0.17	0.24	0.68	0.67	0.7	0.7	0.77	0.81	0.81	0.98	1	0.82	0.85	0.93	0.95
IDL_C	0.11	0.14	0.21	0.66	0.63	0.67	0.65	0.77	0.8	0.86	1	0.98	0.8	0.8	0.92	0.91
S_ldlc_semi	0.03		0.13	0.75	0.55	0.62	0.87	0.92		1	0.86	0.81	0.88	0.85	0.89	0.85
S_ldlc	0.13	0.08	0.1	0.52	0.52	0.54	0.8	0.91	1		0.8	0.81	0.73	0.74	0.8	0.8
S_totalc	0.38	0.08	0.13	0.65	0.7	0.71	0.79	1	0.91	0.92	0.77	0.77	0.7	0.73	0.77	0.78
S_ApoB	0.07	0.14	0.11	0.43	0.48	0.48	1	0.79	0.8	0.87	0.65	0.7	0.63	0.67	0.67	0.7
TotCho	0.49	0.13	0.34	0.88	0.98	1	0.48	0.71	0.54	0.62	0.67	0.7	0.69	0.73	0.72	0.75
PC	0.54	0.16	0.33	0.8	1	0.98	0.48	0.7	0.52	0.55	0.63	0.67	0.62	0.67	0.66	0.7
SM	0.34	0.09	0.31	1	0.8	0.88	0.43	0.65	0.52	0.75	0.66	0.68	0.77	0.79	0.77	0.77
Alb	0.09	0.28	1	0.31	0.33	0.34	0.11	0.13	0.1	0.13	0.21	0.24	0.36	0.37	0.31	0.32
Phe	−0.01	1	0.28	0.09	0.16	0.13	0.14	0.08	0.08		0.14	0.17	0.17	0.19	0.17	0.19
S_ApoA1	1	−0.01	0.09	0.34	0.54	0.49	0.07	0.38	0.13	0.03	0.11	0.09	0.04	0.06	0.08	0.09

Figure S6. (**A**) The pairwise correlation (Pearson R) of the 16 traits that were significantly associated with *ALB* deletion. The cells shown in gray represent missing data, since the S_ldlc_semi trait (serum LDL cholesterol in semi-fasting samples) shared zero samples with S_ldlc (serum LDL cholesterol in fasting samples) and Phe (phenylalanine). **(B)** Comparison of the association p-value of the *ALB* deletion and the 16 traits, with (y-axis) and without (x-axis) albumin (top) and total cholesterol (bottom) as a covariate. The increases of significant level of most traits when conditioned on albumin were likely due to Berkson's paradox[1].

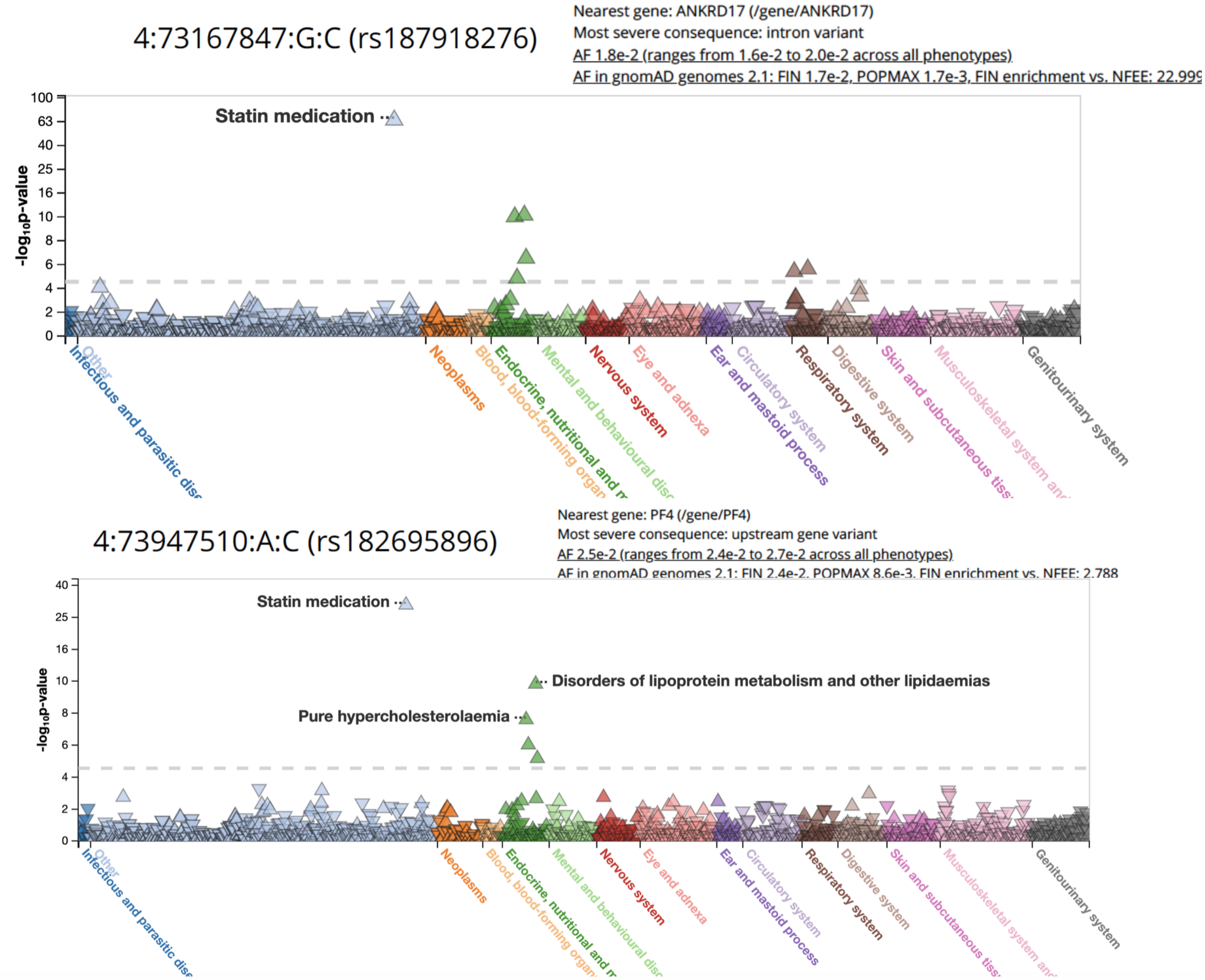

Nearest gene: ANKRD17 (/gene/ANKRD17)
Most severe consequence: intron variant
AF 1.8e-2 (ranges from 1.6e-2 to 2.0e-2 across all phenotypes)
AF in gnomAD genomes 2.1: FIN 1.7e-2, POPMAX 1.7e-3, FIN enrichment vs. NFEE: 22.99

Nearest gene: PF4 (/gene/PF4)
Most severe consequence: upstream gene variant
AF 2.5e-2 (ranges from 2.4e-2 to 2.7e-2 across all phenotypes)
AF in gnomAD genomes 2.1: FIN 2.4e-2, POPMAX 8.6e-3, FIN enrichment vs. NFEE: 2.788

4:73167847:G:C (rs187918276)
-log₁₀p-value
100
63
40
25
16
10
8
6
4
2
0
Statin medication
Other
Infectious and parasitic dise
Neoplasms
Blood, blood-forming organ
Endocrine, nutritional and m
Mental and behavioural diso
Nervous system
Eye and adnexa
Ear and mastoid process
Circulatory system
Respiratory system
Digestive system
Skin and subcutaneous tiss
Musculoskeletal system and
Genitourinary system
4:73947510:A:C (rs182695896)
-log₁₀p-value
40
25
16
10
8
6
4
2
0
Statin medication
Disorders of lipoprotein metabolism and other lipidaemias
Pure hypercholesterolaemia
Other
Infectious and parasitic dise
Neoplasms
Blood, blood-forming organ
Endocrine, nutritional and m
Mental and behavioural diso
Nervous system
Eye and adnexa
Ear and mastoid process
Circulatory system
Respiratory system
Digestive system
Skin and subcutaneous tiss
Musculoskeletal system and
Genitourinary system

Figure S7. Screenshots from the FinnGen PheWeb browser[2] (Data Freeze 3) of the top tagging SNP for the *ALB* deletion (top) and for the cholesterol candidate (bottom) predicted by fine mapping with CAVIAR, showing the phenome-wide association results for each of the SNPs, colored by phenotype groups.

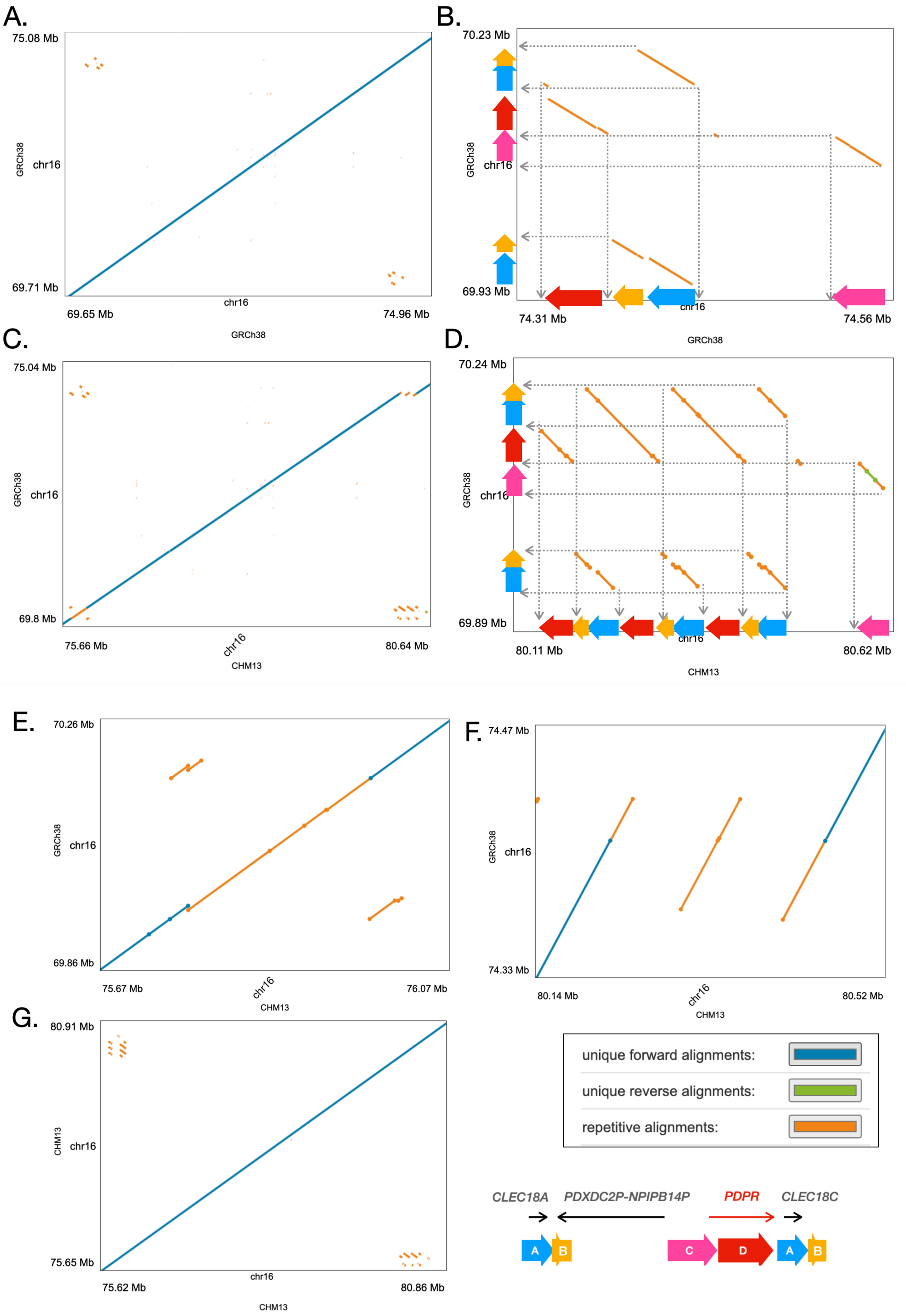

Figure S8. Dot plots showing the structure of the *PDPR* and nearby pseudogene locus in both the GRCh38 and CHM13 assemblies, with repetitive alignments shown in orange and unique alignments shown in blue and green (see legend bottom right). **(A)** The *PDPR* locus in GRCh38 (y-axis) aligned to the pseudogene locus (x-axis) in GRCh38, where **(B)** shows a zoomed-in version with the diagram used for **Figure 4** using the same colors and letter. **(C)** and **(D)** show the *PDPR* locus in GRCh38 vs.

the *PDPR* locus in CHM13. **(E)** and **(F)** show the pseudogene locus in GRCh38 vs. CHM13, and **(g)** shows the *PDPR* locus in CHM13 vs. itself.

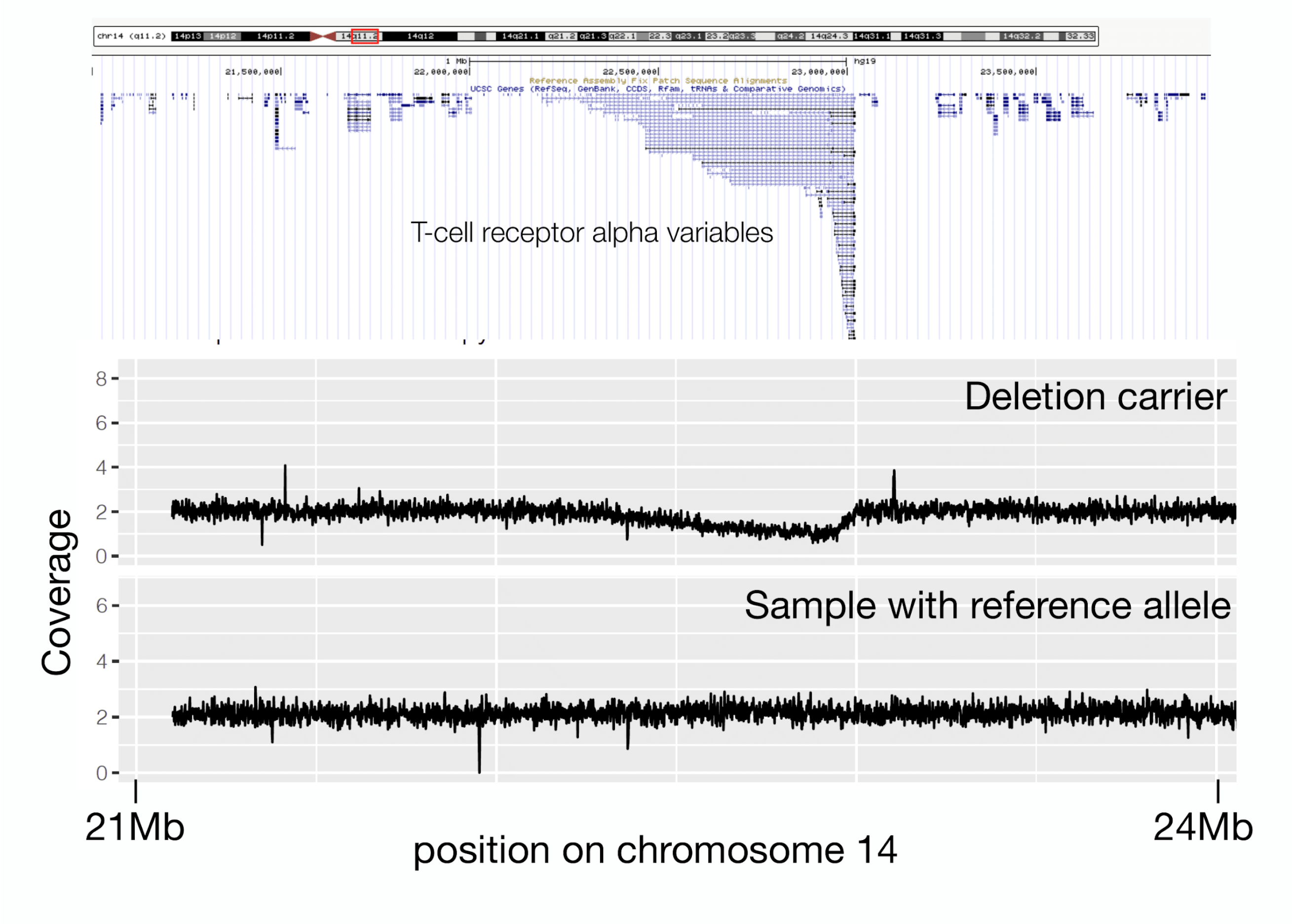

Figure S9. Read-depth coverage patterns at the chr14 T-cell receptor alpha variable region (coordinates LiftOver to GRCh37/hg19), showing one example for “deletion” carriers and one for a sample with the reference allele. The coverage values were calculated by CNVnator for 100bp windows, and the top gene track was extracted from UCSC genome browser (GRCh37/hg19).

Supplemental Tables

Table S1. Variant and sample counts in each QC step for WGS data.

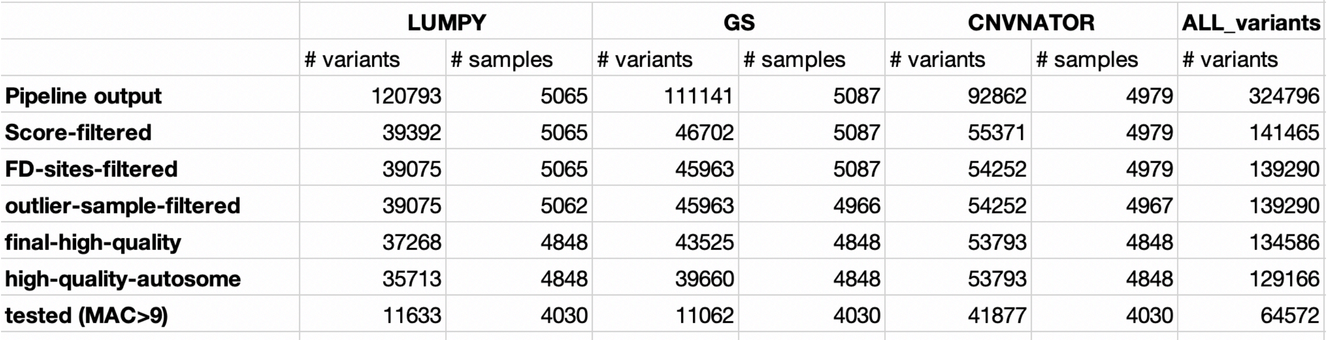

	LUMPY		GS		CNVNATOR		ALL_variants
	# variants	# samples	# variants	# samples	# variants	# samples	# variants
Pipeline output	120793	5065	111141	5087	92862	4979	324796
Score-filtered	39392	5065	46702	5087	55371	4979	141465
FD-sites-filtered	39075	5065	45963	5087	54252	4979	139290
outlier-sample-filtered	39075	5062	45963	4966	54252	4967	139290
final-high-quality	37268	4848	43525	4848	53793	4848	134586
high-quality-autosome	35713	4848	39660	4848	53793	4848	129166
tested (MAC>9)	11633	4030	11062	4030	41877	4030	64572

Table S1. Variant and sample counts in each QC step for WGS data separated by variant calling pipelines. FD – false discovery, see **Methods** for the filtering criteria in each step.

Table S2. Genotype redundancy estimation

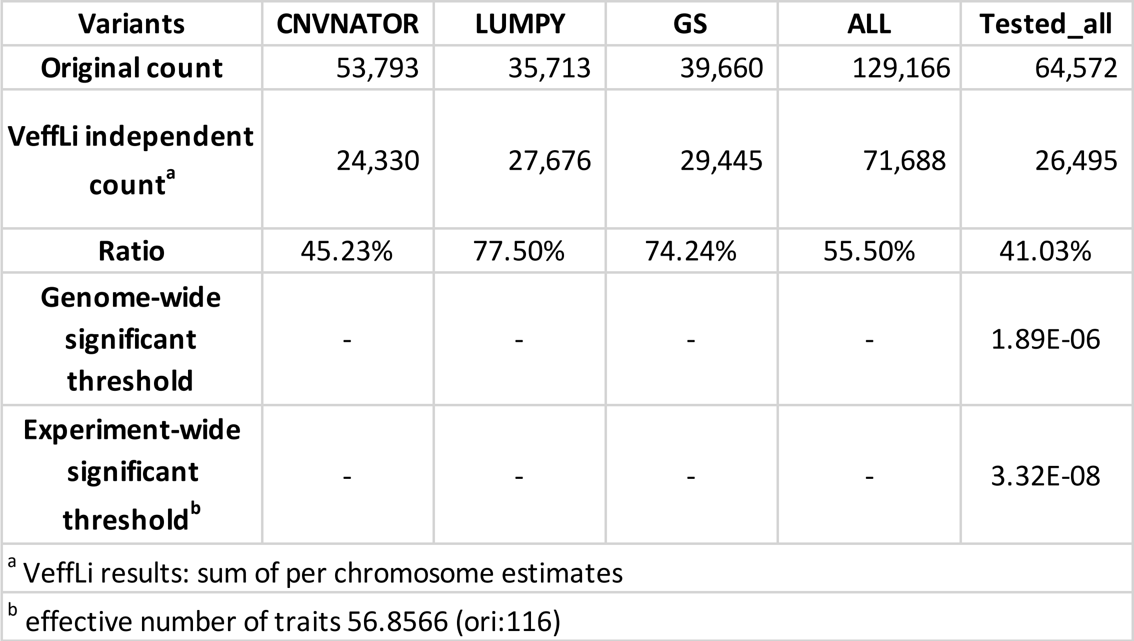

Variants	CNVNATOR	LUMPY	GS	ALL	Tested_all
Original count	53,793	35,713	39,660	129,166	64,572
VeffLi independent count[a]	24,330	27,676	29,445	71,688	26,495
Ratio	45.23%	77.50%	74.24%	55.50%	41.03%
Genome-wide significant threshold	-	-	-	-	1.89E-06
Experiment-wide significant threshold[b]	-	-	-	-	3.32E-08

[a] VeffLi results: sum of per chromosome estimates

[b] effective number of traits 56.8566 (ori:116)

Table S2. Estimation of redundant SV calls based on genotype information. Redundant variant calls identified by multiple SV detection methods are expected to have genotypes that are highly correlated. We therefore applied matSpDlite to each pipeline and to the combined callset to calculate the numbers of independent makers (VeffLi). We then applied the same method to the subset of the variants included in the trait association test and to the phenotypes to perform Bonferroni correction for the genome-wide significance threshold and experiment-wide threshold.

Table S3. Fragmentation level

Pipeline	#. SV	# Cluster	average cluster size	% single variant cluster	size of the largest cluster
GS	39,660	24,497	1.619	75%	96
LUMPY	35,713	23,751	1.321	90%	458[a]
LUMPY CNV	27,858	21,759	1.28	90%	149
CNVNATOR	53,793	16,962	3.171	73%	527

[a] a large inversion on chr7 with size of 44mb covered 400+ other variants

Table S3. Estimation of SV fragmentation based on physical clustering. Due to coverage fluctuations, CNV calls detected by read-depth analysis are often fragmented into multiple adjacent CNV calls that in fact represent a single variant. To estimate the degree of fragmentation, we clustered high-confidence autosomal CNVs within 10bp of each other and calculated the average number of SVs per cluster (average cluster size), the percentage of single variant clusters, and the maximum number of variants per cluster (size of the largest cluster).

Table S4. Leave-one-out validation for genome-wide significant SVs

VAR	FALSE	TRUE	AC_RATE
40551	17	3891	0.996
52933	113	3795	0.971
61703	55	3853	0.986
62003	7	3901	0.998
chr12_95946601_95947800	260	3648	0.933
chr16_72057601_72058200	63	3845	0.984
chr20_45906701_45907200	144	3764	0.963
CNV_chr4_73399922_73404147	9	3899	0.998

Table S4. The “leave-one-out” validation experiment to assess imputation quality of the eight genome-wide significant SVs. For each variant, we ran 3,908 imputation experiments and in each we used one sample as the test genome and the other samples as the reference. The accuracy rate was calculated among all 3,908 tests.

Table S5. Summary statistics for all genome-wide significant signals, before manually clumping redundant variants into single calls. P-value (P), effect size (BETA), allele count (AC), allele frequency (AF) and sample size (N) are shown for whole genome (WGS), exome (WES) and imputed (IMP) data. The combined p-value (COMBINED_P) was calculated using Fisher’s method. The WES_I_SQUARE (%) column was a heterogeneity statistics provided from the meta-analysis of the two WES batches.

Table S6. Test ALB deletion conditioned on GWAS SNPs

rs ID	GWAS trait	First author, year	R2 w. SV	MAF (Finns)	MAF (Reported)	SV P value		Beta (conditional	
						albumin ~ SNP + SV	cholesterol ~ SNP + SV	albumin	cholesterol
rs16850360	albumin	Kettunen et al, 2012 Inouye et al, 2012	0.3	0.025	0.03	8.10E-18	6.00E-04	1.1	-0.39
rs182616603	cholesterol	Surakka et al, 2015	0.3	0.024	0.01	6.60E-17	4.00E-03	1.06	-0.32
rs2168889[a]	albumin	Inouye et al, 2012	0.12	0.049	0.05	6.40E-23	9.70E-05	1.05	-0.37
rs1851024	albumin	Inouye et al, 2012	0.08	0.049	0.05	2.30E-19	3.30E-08	0.91	-0.5
rs117087731	cholesterol	Surakka et al, 2015	6.00E-04	0.02	0.01	2.50E-21	1.70E-08	0.91	-0.49
rs115136538	albumin	Kettunen et al, 2012	3.00E-05	0.005	0.02	2.80E-21	1.50E-08	0.91	-0.49
rs184650103	albumin	Kettunen et al, 2016	3.00E-05	0.001	0.01	2.90E-21	1.60E-08	0.91	-0.49
rs182695896[b]	.	.	0.49	0.024	.	6.52E-13	2.33E-02	0.97	-0.27

SV ~ albumin P value = 3.49E-21, beta = 0.9107

SV ~ cholesterol P value = 1.17E-08, beta = -0.4929

[a] rs2168889: collider effect

[b] rs182695896: top causal candidate for cholesterol in our study, has not reported in published GWAS papers

Table S6. Association analysis between the *ALB* deletion and albumin/total cholesterol conditioned on the seven previously published GWAS SNPs and rs182695896 one at a time. None of the seven GWAS SNPs diminish the SV-albumin signal, while the first three SNPs attenuate the SV-cholesterol signal, suggesting that they might also be in LD with the underlying causal variants for cholesterol. MAF(Finns) – MAF in our data, MAF(Reported) – MAF reported in previous GWAS studies.

Table S7. Test the GWAS SNPs w./w.o. SV as covariate

rs ID	GWAS trait	First author, year	R2 w. SV	MAF (Finns)	MAF (Reported)	SNP P value		Beta (alb)	SNP P value		Beta (chol)
						albumin ~ SNP	albumin ~ SNP + SV		cholesterol ~SNP	cholesterol ~SNP + SV	
rs16850360	albumin	Kettunen et al, 2012 Inouye et al, 2012	0.3	0.025	0.03	2.30E-06	0.05	-/+	2.90E-06	0.18	+/+
rs182616603	cholesterol	Surakka et al, 2015	0.3	0.024	0.01	1.40E-06	0.08	-/+	5.30E-08	0.020	+/+
rs2168889	albumin	Inouye et al, 2012	0.12	0.049	0.05	>0.05	-	-	4.40E-07	0.002	+/+
rs1851024	albumin	Inouye et al, 2012	0.08	0.049	0.05	2.20E-03	0.83	+/+	>0.05	-	-
rs117087731	cholesterol	Surakka et al, 2015	6.0E-04	0.02	0.01	>0.05	-	-	>0.05	-	-
rs115136538	albumin	Kettunen et al, 2012	3.0E-05	0.005	0.02	>0.05	-	-	>0.05	-	-
rs184650103[a]	albumin	Kettunen et al, 2016	3.0E-05	0.001	0.01	NA	NA	NA	NA	NA	NA
rs182695896[b]	.	.	0.49	0.024	.	6.65E-10	0.56	-/+	6.18E-09	0.0096	+/+

[a] rs184650103 was too rare to be included in the test, so the summary statistics were marked as “NA”, to differentiate from “-”, which marks non-significant S

[b] rs182695896 was the top causal candidate for cholesterol in our study, has not reported in published GWAS papers

Table S7. The association tests between each of the seven previously published GWAS SNPs as well as rs182695896 and serum albumin/total cholesterol, with and without the *ALB* deletion as a covariate (SNPs with p-value > 0.05 were not included in the conditional analysis, with “-” in the related fields). The “Beta” column shows the direction of effects of SNPs with/without the SV in the model. rs115136538, rs184650103 and rs117087731 did not show significant association with either trait in our dataset. The other SNPs showed signals with albumin or total cholesterol which became much less

significant after conditioning on SV genotype. *Note: rs184650103 was too rare to be included in the test, so the summary statistics were marked as “NA”, to differentiate from “-”, which marks non-significant SNPs.

Table S8. Conditional analysis (phenotype - phenotype)

Variant	Tested trait	Covariate trait	P WGS	P conditioned	BETA WGS	BETA conditioned	Mediator?
ALB deletion	Albumin	Total Cholesterol	3.49E-21	5.74E-25	0.9107	0.9937	N
	Total cholesterol	Albumin	1.17E-08	1.16E-11	-0.4929	-0.6558	N
PDPR mCNV	Pyruvate	Alanine	9.41E-11	6.59E-05	-0.5817	-0.4344	N
	Alanine	Pyruvate	2.93E-07	1.47E-03	-0.5744	-0.3197	Y
HP deletion	Glycoprotein	Total cholesterol	1.51E-11	2.78E-15	-0.2081	-0.1988	N
	Total cholesterol	Glycoprotein	1.01E-05	2.62E-10	0.1466	0.1604	N

Table S8. Conditional analysis of the three multi-trait associated variants, taking one trait as a covariate and testing the other. Additional traits were tested for the *ALB* deletion conditioned on albumin and total cholesterol, the results of which can be found in **Supplementary Figure 6b**. The covariate trait was defined as a mediator of the tested trait if the conditional p-value failed the genome-wide significance threshold (1.89×10^{-6}).

Table S9. High-confidence autosomal SVs count

Type	GenomeSTRiP	LUMPY	CNVnator	Total
DEL	16,793	22,856	15,424	55,073
DUP	14,076	5,002	13,312	32,390
BND	-	4,337	-	4,337
INV	-	187	-	187
MEI	-	3,331	-	3,331
mCNV	8,791	-	25,057	33,848
ALL	39,660	35,713	53,793	129,166

Table S9. Count of high-confidence autosomal SVs stratified by variant type and detection method including deletions (DEL), duplications (DUP), multiallelic copy number variants (mCNV), inversions (INV), mobile element insertions (MEI) and generic rearrangements of unknown architecture (BND).

Supplemental References

1. Berkson, J. (1946). Limitations of the Application of Fourfold Table Analysis to Hospital Data. Biometrics Bulletin *2*, 47.

2 .FinnGen project PheWeb: http://r4.finngen.fi/about